Joint Pathology Center
Veterinary Pathology Services

WEDNESDAY SLIDE CONFERENCE
2020-2021

Conference 6

30 September 2020

Joint Pathology Center
Silver Spring, Maryland

CASE 1: N16-032 (4084301-00)

Signalment: 13 yrs of age, spayed female, Golden Retriever, *Canis lupus familiaris*, canine.

History:
It was reported that the patient had decreased appetite and lethargy for the past 1-2 weeks and had diarrhea for ~1 day. She had a history of seizures for the past ~3 years; her last seizure was 1 month ago. The patient had a generalized lymphadenopathy (lymphoma). Patient was on phenobarbital, was obese and was 5-7% dehydrated.

Gross Pathology:
Relevant gross pathologic findings included: Multiple (n=10) well-demarcated, unattached, soft, white, lipid-like masses (lipomas) ranging from 4-20 cm in diameter, were present in the subcutis. There was generalized enlargement of peripheral lymph nodes ~4 times larger than normal. The left caudal lung lobe had a 1 cm focal firm, dark red area of depression. The right ventricular free wall was 3 mm and the left was 7 mm (right:left ratio of 1:2.3). The right and left kidney contained innumerable miliary white foci throughout the cortical parenchyma. A 3mm cyst was present on the cortical surface of the right kidney. The parietal lobe of the left cerebral hemisphere was depressed by an approximately 2.2x1.5x2 cm firm mass originating from the dura mater (meningioma).

Laboratory results:
Cytology: It was reported that ante-mortem cytology of blood smears from this animal were consistent with lymphoid leukemia.
Special staining: Under polarized light, Congo Red special stain revealed apple-green birefringence of material effacing glomeruli and cardiac vessel.

Microscopic description:
The microscopic findings for the submitted tissues are:

Kidneys: Glomeruli are diffusely and globally obscured and expanded by amorphous homogenous pale eosinophilic to amphophilic material (amyloid). Bowman's capsules are variably thickened and there is marked synechia

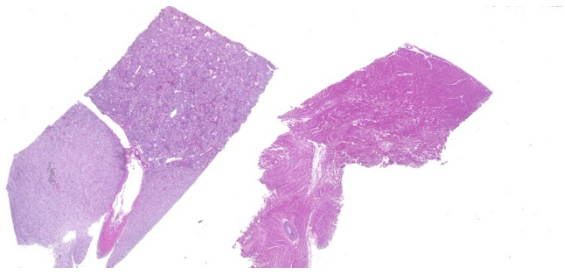

Kidney, heart, dog. One section of kidney and heart are submitted for examination. (HE, 5X)

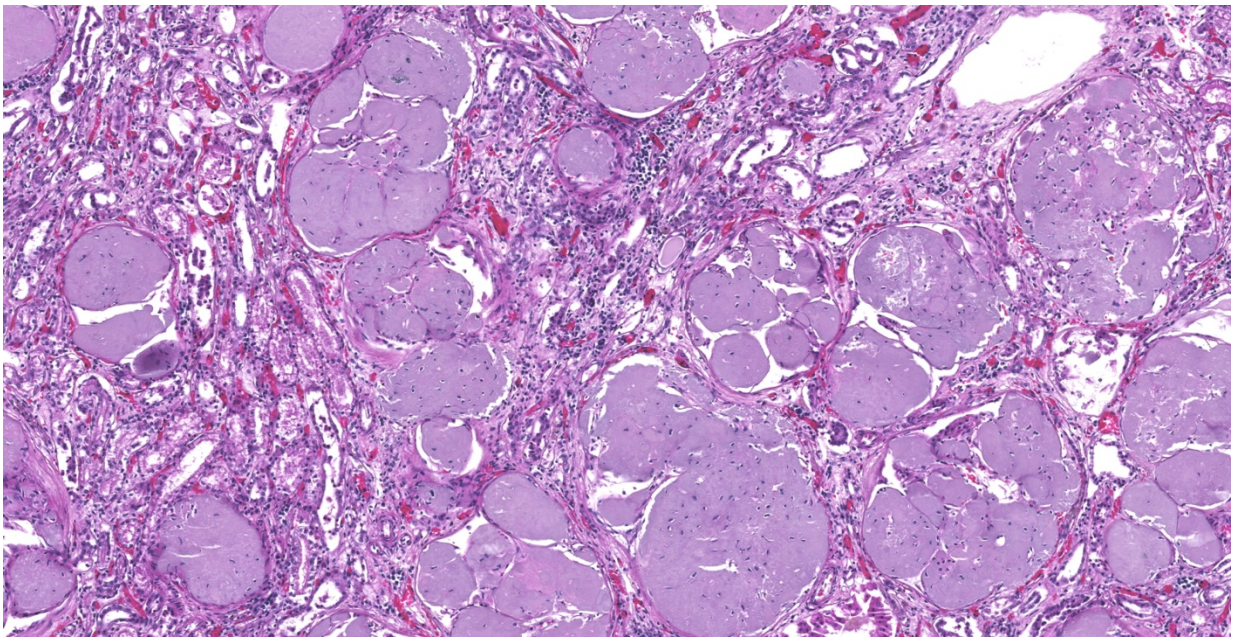

Kidney, dog. Glomeruli are diffusely and globally expanded by amyloid, and there is a marked loss of tubules within the intervening parenchyma. Moderate numbers of the lymphocytes and plasma cells are present within the interstitium. (HE, 100X)

formation. The interstitium is diffusely infiltrated with small to moderate amounts of lymphocytes and plasma cells.

Heart: Arteries and arterioles throughout the myocardium frequently have transmural thickening of the vessel wall by amorphous pale amphophilic material (amyloid). Affected vessels often have recanalization characterized by multiple small caliber spaces. There is marked endocardial fibrosis and few scattered multifocal areas of mild to moderate interstitial fibrosis; associated cardiac myocytes are shrunken and fragmented (degeneration). There are also a few multifocally extensive areas of myocardial loss and replacement by adipose tissue and scattered macrophages, lymphocytes and plasma cells.

Contributor's morphologic diagnosis:
Kidney: Severe diffuse global glomerular amyloidosis
Heart: Submassive severe coronary arterial wall amyloidosis with recanalization
Heart: Moderate multifocal interstitial myocardial fibrosis and fatty infiltration with myocardial degeneration.

Morphologic diagnoses for tissues not submitted:
Meninges: Meningioma
Brain: Meningioma-associated cerebrocortical compression with locally extensive astrocytosis, oligodendrogliosis, neuronal satellitosis and periglial edema
Lymph node and Spleen: Metastasis of lymphoid leukemia
Lung: Focal bronchioloalveolar carcinoma, well-differentiated

Contributor's comment:
The animal in this case had multiple neoplastic processes. The neoplastic leukemic lymphoid cells were effacing the lymph nodes, in pericapsular vessels associated with lymph nodes and multifocally present in the spleen. This neoplasm is considered the primary cause of illness in this case. The meningioma and its compression against the parietal lobe of the brain resulted in seizures. There was also a well-differentiated bronchioloalveolar carcinoma identified in one site in the lung.

Amyloidosis can be secondary to chronic inflammatory or neoplastic processes; considering the multiple neoplasms in this case,

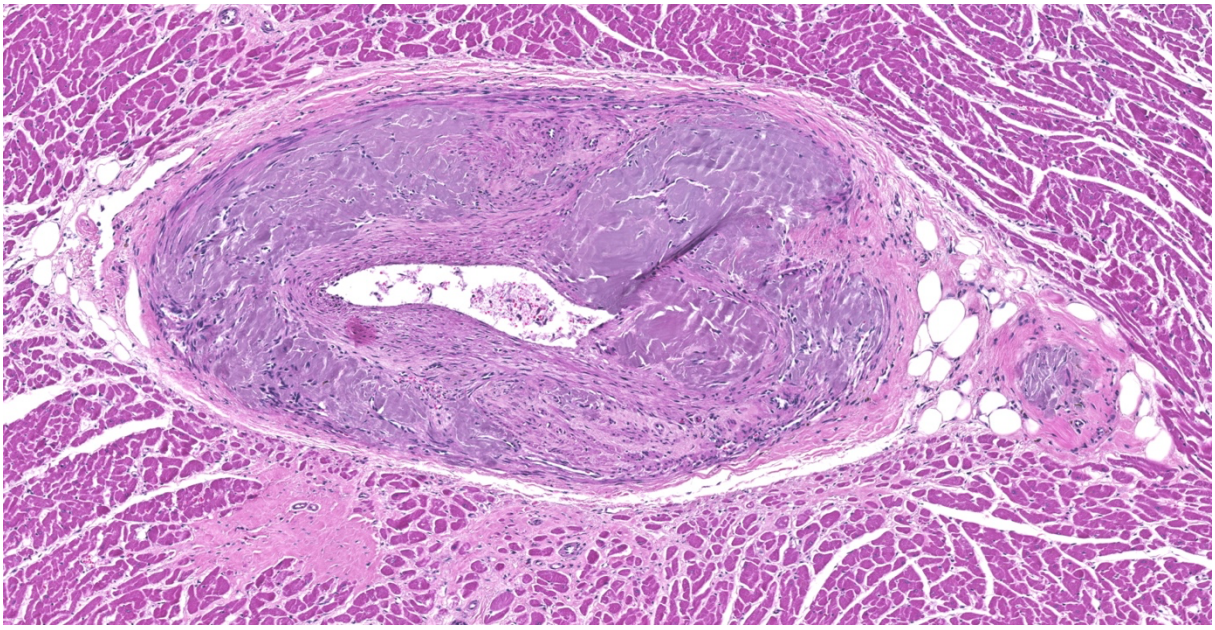

Heart, dog. The walls of myocardial arteries are multifocally expanded by amyloid which encroaches on the lumen. There is moderate fibroplasia of the adjacent arterial wall and periarteriolar fibrosis. There is loss of myofibers and replacement fibrosis in the adjacent myocardium. (HE, 97X)

including lymphoid leukemia, it is likely that the amyloid deposition in the kidney, and possible the myocardial vasculature as well, was secondary to other disease processes going on. The amyloid deposition in the vessels of the heart may also be secondary to aging, as senile amyloid plaques have been reported in muscular arteries of the myocardium, lungs, and spleen of old dogs. The cause of the myocardial lesions may be secondary to the vascular amyloidosis in the heart and impaired oxygenation of the associated musculature.

The term amyloid refers to a group of glycoproteins whose protein components represent β-pleated sheet patterns. In a healthy patient, the immune system is usually able to either repair (chaperones) or degrade (ubiquitin-proteosome pathway) these proteins. However, if the body is unable to perform such feats, one can end up with amyloidosis. These proteins deposit into organs and result in pressure atrophy of adjacent cells as they accumulate.

Amyloidosis can be classified into systemic (amyloid deposits in multiple organs) and localized (single organ) amyloidosis, and further categorized into primary and secondary amyloidosis. Primary amyloidosis, which is associated with the amyloid light chain (AL form), is the most common form in humans, while secondary amyloidosis, which is associated with the amyloid-associated (AA) form, is most common in animals.

The AL form is immunoglobulin-derived and can be deposited by B lymphocytes as well as plasma cells and result from immunocyte dyscrasias. The AA form of amyloidosis is derived from the

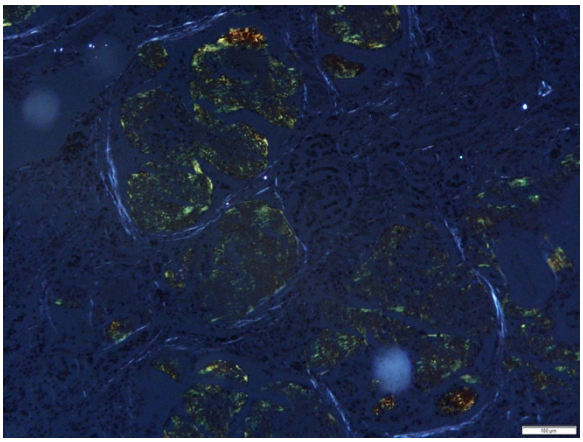

Kidney, dog. Under polarized light, Congo Red histochemical stain reveals apple-green birefringence of amyloid effacing glomeruli. (Congo Red, 10X) (Photo: Courtesy of Tuskegee University College of Veterinary Medicine)

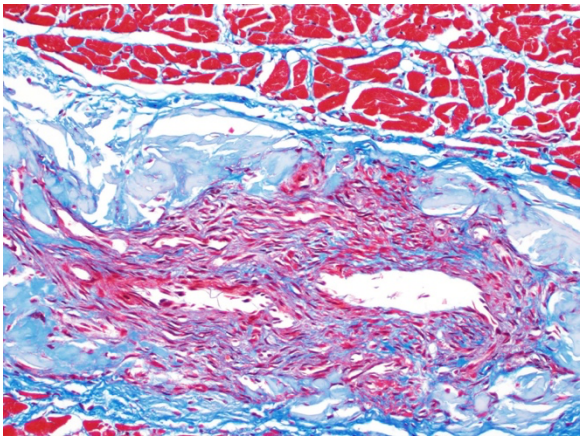

Heart dog. A Masson's trichrome demonstrates the mural fibroplasia surrounding amyloid plaques in affected arterioles. (Masson's trichrome, 100X)

precursor serum-amyloid associated (SAA) protein. This precursor is synthesized in the liver and its production is increased in pro-inflammatory states such as chronic inflammation and neoplasia. With the lack of proteolytic action on these proteins, amyloidosis can result. Humans have these same two forms, as well as the β-amyloid form (Aβ) which is found in the cerebral plaques of Alzheimer patients. Other less common forms of amyloidosis in animals is islet amyloid polypeptide (IAPP) produced in pancreatic islets of cats with non-insulin-dependent diabetes mellitus and apolipoprotein AI (apoAI) amyloidosis deposited in pulmonary vessels of aged dogs.

The kidney is the most common site for deposition of AA amyloid in association with other disease. In dogs, localization to glomeruli is most common. In contrast, in cats and Chinese Shar-Pei dogs with renal amyloidosis, the amyloid is usually localized to the renal medulla. Clinical pathologic parameters frequently associated with glomerular amyloidosis include proteinuria and may progress to nephrotic syndrome. With medullary amyloidosis, the amyloid becomes obstructive in nature resulting in capillary and tubular basement membrane obstruction and thickening, papillary necrosis and medullary interstitial fibrosis. A hereditary predisposition to AA amyloidosis (familial amyloidosis) has been described in Abyssinian cats and Chinese Shar-Pei dogs.

The amyloid that was found in the cardiac vessels of this animal may be due to the systemic disease affecting this dog but may also be associated to aging. Cardiac amyloidosis has been reported in dogs ≥7 years and is somewhat comparable to the senile cardiac amyloidosis of humans, which is seen in those age 70 and greater. A prominent difference is that amyloid builds up in the atria and ventricles of the heart in humans, while studies show that it primarily only affects arterioles in dogs.[2]

Grossly, amyloidosis can be diagnosed by using Lugol's agent followed by diluted sulfuric acid. If the tissue becomes a purple to dark blue tinge, it is positive for amyloidosis. Microscopically, one could use Congo Red stain as well as thioflavine-T. The stain itself is not taken up by the protein, but rather caught in the β-pleated sheet. Under polarized light, the amyloid proteins emit an apple-green birefringence with the Congo Red. In the case of AA amyloidosis, the addition of potassium permanganate results in the loss of the Congo Red stain, enabling differentiation from the AL form of amyloidosis. Thioflavine-T is bright yellow under fluorescent light and may be more sensitive than Congo Red. Utilizing electron microscopy, amyloid fibrils are characterized by 7.5-10 nm diameter, nonbranching tubules.

Contributing Institution:
Tuskegee University College of Veterinary Medicine
1200 West Montgomery Road
Tuskegee, AL 36088
http://www.tuskegee.edu/academics/colleges/cvmnah/school_of_veterinary_medicine.aspx

JPC diagnosis:

1. Kidney: Amyloidosis, glomerular, global, diffuse, severe, with tubular degeneration and loss, and chronic interstitial nephritis, golden retriever, canine.
2. Heart: Amyloidosis, arterial, diffuse, severe, with multifocal myofiber atrophy, loss, and fibrosis.

JPC Comment: The contributor describes amyloidosis in detail, and the methods of detection remain the most accessible in the field.

Amyloidosis documented in a wide range of wild and captive mammals and birds.[5] While there are many fewer documented cases, reptiles with cases of systemic amyloidosis have been documented within the last three years. A 12-year-old male African tiger snake with concurrent *Mycobacterium avium-intracellulare* complex infection, biliary cystadenocarcinoma, with intrahepatic metastases had splenic amyloidosis with amyloid also present in testicular interstitium and occasional blood vessel walls. Mycobacteriosis is a common cause of reactive amyloidosis, and the serum amyloid A (SAA) gene is highly conserved across species.[1]

A strain of mouse designated *App*$^{NL\text{-}G\text{-}F/NL\text{-}G\text{-}F}$ has been bred with three distinct introduced mutations that increase production of amyloid precursor protein (APP), which results in reliable overproduction of amyloid β and histologic and clinical signs consistent with Alzheimer's disease. Based on examination of the non-cognitive, emotional domains of these mice, they serve as a useful model of preclinical Alzheimer's disease in humans.[4]

Human cardiac light chain (AL) amyloidosis is a particularly lethal disease, responsible for approximately 75% of mortality associated with AL amyloidosis. Zebrafish were altered to selectively secrete human λ-light chain proteins in the liver, which were then exported to systemic circulation. These zebrafish developed cardiomyopathies consistent with early cardiac AL amyloidosis, and may represent a future animal model of the human disease.[3]

References:

1. Burns RE, Gaffney PM, Nilsson KPR, Armien AG, Pessier AP. Systemic amyloidosis in an African Tiger Snake (*Telescopus semiannulatus*). *J Comp Path*. 2017;157:136-140.
2. Jonsson, L., *Senile cardiac amyloidosis in the dog.* Acta Vet Scand, 1974. **15**(2): p. 206-18.
3. Mishra S, Joshi S, Ward JE, et al. Zebrafish model of amyloid light chain cardiotoxicity: regeneration vs degeneration. *Am J Physiol Heart Circ Physiol*. 2019;316(5):H1158-H1166.
4. Sakakibara Y, Sekiya M, Saito T, Saido T, Iijima KM. Cognitive and emotional alterations in App knock-in mouse models of Aβ amyloidosis. *BMC Neurosci*. 2018;19:46.
5. Terio KA, McAloose D, St. Leger J. *Pathology of Wildlife and Zoo Animals*. Elsevier: San Diego, CA. 2018.

CASE 2: 13-6752 (4048083-00)

Signalment: Two-month-old female Galloway cross calf.

History: This calf was from a group of about 100 Galloway and Galloway cross calves. One calf died 3 weeks previously but was not autopsied, and calves were treated for coccidia with sulfa boluses at that time. This calf had been sick for 1-2 days, exhibiting lethargy and dyspnea leading to lateral recumbency and death. The autopsy was performed shortly after death by the referring veterinarian.

Gross Pathology: No icterus was noted. The liver and spleen were noted to be yellow-grey and

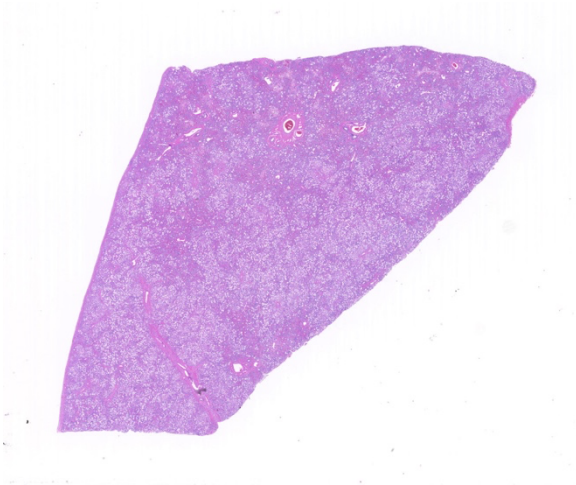

Liver, ox. Subgross examination of the submitted section of liver demonstrates a retiform pattern of pallor. (HE, 5X)

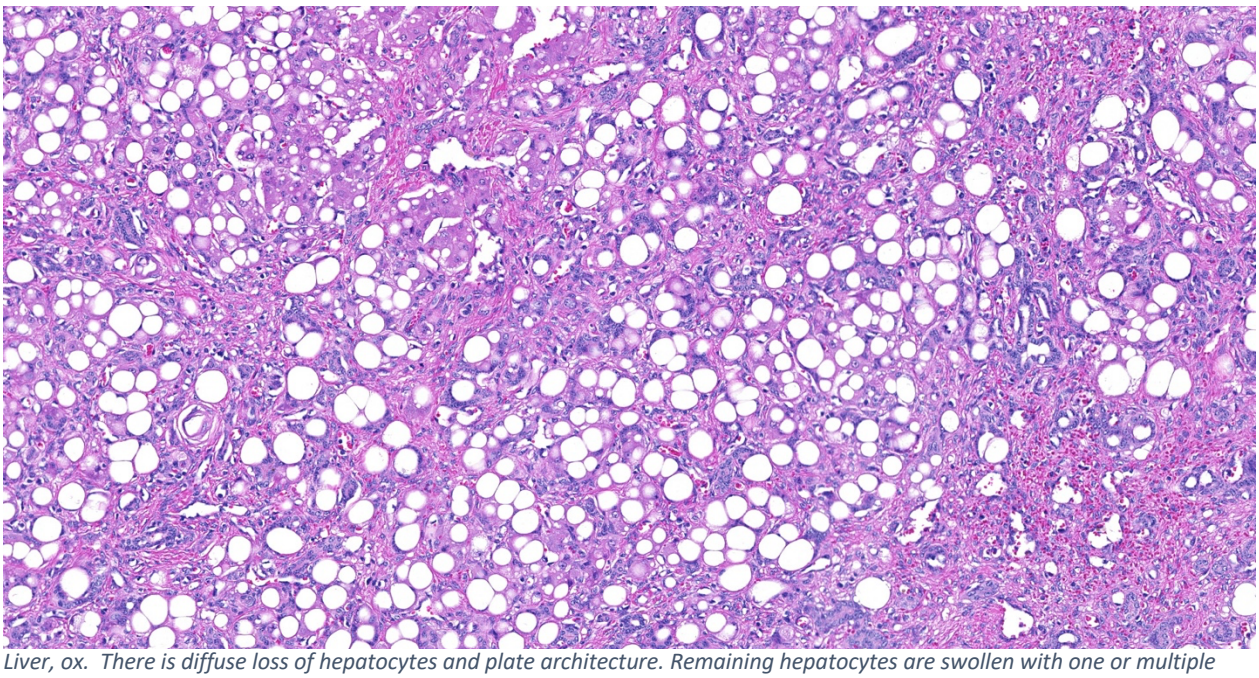

Liver, ox. There is diffuse loss of hepatocytes and plate architecture. Remaining hepatocytes are swollen with one or multiple lipid vacuoles, and there is fibrosis and biliary duplication within all parts of the lobule. (HE, 135X)

did not bleed when cut. Only liver was submitted for histopathology.

Laboratory results: A postmortem blood sample was noted to have lipemic serum. PCV = 60%, total protein = 6.8. A fecal float was negative for parasite eggs.

Microscopic description:
In representative sections of liver, the hepatic lobular organization and microanatomy were severely disrupted by fibrosis interspersed with bile ductules which dissected through all levels of the lobule and segregated the hepatocytes into variably sized nodules. The central veins were ill-defined and randomly located. The hepatocytes within the nodules were variably sized and contained large, clear, intracytoplasmic vacuoles that displaced the nucleus peripherally. Portal areas were markedly expanded by large amounts of fibrous connective tissue and multiple bile ductules, and the tunica media of the hepatic, portal and central veins were severely thickened by fibrous tissue with collapse of the vascular lumens. Hepatic sinusoids were tiny or absent and not contiguous.

Contributor's morphologic diagnosis:
Diffuse, severe, chronic hepatocellular lipidosis with severe periportal fibrosis and bile duct hyperplasia.

Contributor's comment:
Lesions were compatible with hepatic lipodystrophy of Galloway cattle. The condition has been diagnosed sporadically in the breed since 1965 but no genetic, metabolic or nutritional cause has been identified to date.[6] In 1999, the clinicopathologic findings in 15 cases from 5 farms in Scotland were documented.[4] Affected animals were usually normal at birth, although an aborted fetus and a stillborn calf had liver lesions similar to older affected calves. Within 2-4 months of birth calves became lethargic and progressed to tremors, seizures, recumbency and death. Significant clinical pathologic abnormalities included hypoalbuminemia, elevated liver enzymes and marked elevation in serum cholesterol, triglycerides and fatty acids. The only gross lesions noted at necropsy were large, pale livers. Histopathology of the liver was as described above; the only other histopathologic lesion was white matter spongiosis attributed to hepatic encephalopathy. No mention was made about the

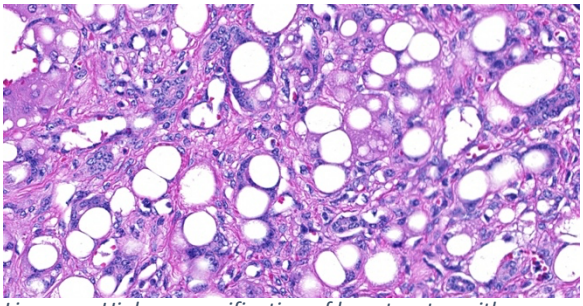

Liver, ox. Higher magnification of hepatocytes with marked lipid vacuolation, fibrosis, and biliary hyperplasia. (HE, 440X)

adequacy of fat stores in the bodies, which may be relevant to human conditions discussed below.

Hepatic lipidosis (or steatosis, in human medical terminology) refers to the excessive accumulation of triglycerides within hepatocytes.[6] The liver's role in fat metabolism is complex and vital, and includes uptake of lipid from plasma chylomicrons, hydrolysis into fatty acids, repackaging via lipoprotein lipase and secretion of very low-density lipoproteins. Excessive storage of lipid as triglycerides in the liver can occur if the supply of lipid exceeds the liver's capacity to process, or if there is a disruption of one or more of the many metabolic steps involved in processing lipid through the peroxisomes and endoplasmic reticulum. In veterinary medicine, hepatic lipidosis can have a variety of pathogeneses, including physiologic (late pregnancy), metabolic (e.g. diabetes mellitus), toxic or nutritional (e.g. ovine white liver disease due to cobalt deficiency). Some conditions, such as ovine white liver, can progress to cirrhosis and liver failure.

In human medicine, lipodystrophies are a large group of rare genetic and acquired diseases characterized primarily by abnormalities in the amount and distribution of adipose tissue.[5] Genetic forms are divided into congenital generalized lipodystrophy and familial partial lipodystrophy. The most common acquired form seen now is in HIV-positive patients treated with protease inhibitors as part of Highly Active Antiretroviral Therapy. Although partial or complete lack of body fat is the primary clinical sign, patients with congenital generalized lipodystrophy have several other clinical manifestations, including early onset hypertriglyceridemia and liver enlargement due to fat accumulation.[2] Insulin resistant diabetes occurs early in life, but cirrhosis develops later. The protein systems defective in all of the reported human congenital and acquired lipodystrophies involve development or processing of lipid droplets within adipocytes.[3] In none of the reviews is there mentioned a form of lipodystrophy with neonatal hepatic steatosis and cirrhosis.

While the disease in Galloway cattle may be a form of lipodystrophy, it does not appear to be a close correlate with any of the human syndromes. It may be more likely to be due to a defect in the liver's capacity to process and release lipids. Clearly more research is required to determine where this fascinating disease fits into the wide spectrum of defects in fat metabolism.

Contributing Institution:
Department of Veterinary Microbiology and Pathology
College of Veterinary Medicine
Washington State University
Pullman, WA 99164-7040

JPC diagnosis:
Liver: Hepatocellular lipidosis, diffuse, severe, with marked hepatocellular loss, fibrosis, and biliary reduplication, Galloway mix, bovine.

JPC comment:
The contributor succinctly illustrates the current understanding of this disease in Galloway cattle. There have been recent case reports in the United Kingdom[7] and Germany, with increasing evidence of a genetic link. In the German herd, 7 calves sired by the same bull were affected, and the herd experienced no further occurrences when the bull was replaced.[9]

Congenital lipodystrophies encompass a variety of rare diseases associated with partial or total absence of normal adipose tissue. One variant, Berardinelli-Seip congenital lipodystrophy (BSCL) is autosomal recessive and has been linked to genetic mutations affecting a lipid biosynthetic enzyme 1-acyl-*sn*-glycerol 3-phosphate *O*-acyltransferase 2 (AGPAT2) or the

integral endoplasmic reticulum membrane protein seipin. A strain of Agpat2 knockout mice have been created to further research of these diseases. At necropsy, *Agpat2*$^{-/-}$ mice are characterized by severe hepatomegaly, complete absence of white adipose tissue, amoeboid adipocytes with microvesiculated basophilic cytoplasm with deficient lipogenesis. Aggregates of brown adipose tissue are smaller and have massive necrosis and early ablation. These mice also have massive pancreatic islet hypertrophy, despite chronic hyperglycemia.[8]

While energy storage is a critical function of adipocytes, they also secrete a variety of hormones (adipokines) such as leptin, adiponectin, TNF-α, IL-6, resistin, and visfatin, all of which play necessary roles in regulating metabolism. With derangement of these adipokines, lipid metabolism becomes incomplete and animals fail to thrive.[8]

Feline hepatic steatosis, feline familial hyperlipoproteinemia, and canine primary idiopathic hyperlipidemia may be closer veterinary correlates to this disease in Galloway calves. The majority of pathologic changes are confined to the liver and involve various aspects of lipid processing ability of hepatocytes. While feline hepatic steatosis is common, the exact mechanism of hepatocellular accumulation of triglycerides remains incompletely described, with a likely multifactorial etiology. In feline familial hyperlipoproteinemia, there is an associated congenital lipoprotein lipase deficiency, leading to lipid vacuoles and ceroid accumulation in hepatocytes, as well as in the spleen, lymph nodes, kidneys, and adrenal glands.[1]

References:

1. Cullen JM, Stalker MJ. Liver and Biliary System. In: Maxie MG ed. Jubb, Kennedy, and Palmer's Pathology of Domestic Animals, Volume 2. 2016:277-278.
2. Garg A, Agrawal A. Lipodystrophies: Disorders of adipose tissue biology. *Biochim Biophys Acta* 2009; **1791**:507-513.
3. Kramer N, Farese Jr RV, Walther TC. Balancing the fat: lipid droplets and human disease. EMBO *Mol Med*. 2013; **5:**905-915.
4. Macleod NSM, Allison CJ. Hepatic lipodystrophy of pedigree Galloway cattle. *Vet Rec.* 1999; **144**:143-145.
5. Nolis T. Exploring the pathophysiology behind the more common genetic and acquired lipodystrophies. J Hum Genet 2014; 59:16-23.
6. Stalker MJ, Hayes AM. Liver and biliary system *In* Pathology of Domestic Animals Fifth edition, ed. M Grant Maxie, Saunders/Elsevier, Edinburgh, 2007, Vol 2, pp 310-315.
7. Strugnell B, Wessels M, Woodger N, et al. Hepatic lipodystrophy of Galloway calves.. Vet Rec. 2015 Sep 12;177(10):265-6.
8. Vogel P, Read R, Hansen G, et al. Pathology of congenital generalized lipodystrophy in *Agpat2*$^{-/-}$ mice. *Veterinary Pathology*. 2011. 48(3):642-654.
9. Weiland M, Mann S, Halfner-Marx A, Ignatius A. Hepatic lipodystrophy in Galloway calves. Veterinary Pathology. 2017;54(3):467-474.

CASE 3: 18/75 (4118754-00)

Signalment: 9 years, female, Flat Coated Retriever dog (*Canis familiaris*)

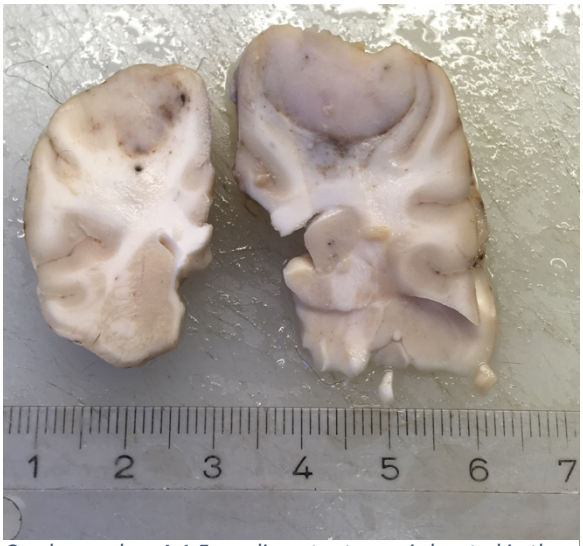

Cerebrum, dog. A 1.5 cm diameter tumor is located in the left hemisphere, compressing adjacent neuroparenchyma. The tumor is well demarcated ventrally but poorly demarcated rostrally and caudally. (Photo courtesy of the Norwegian University of Life Sciences, Oslo, Norway)

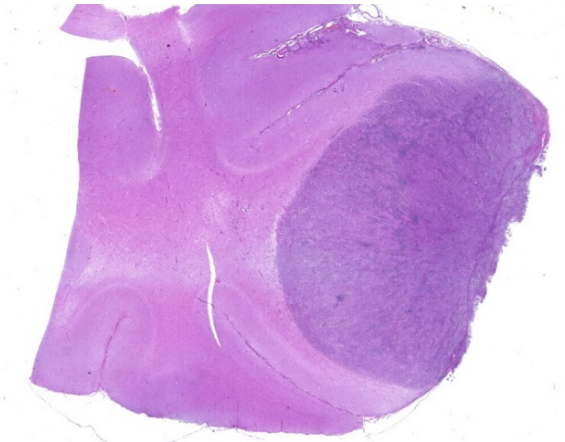

Cerebrum, dog. A 1.5cm nodular densely cellular neoplasm effaces cerebral parenchyma. (HE, 7X)

History:

A week prior to euthanasia, the dog had problems keeping up with the owner on a run. Five days later the dog got generalized tonic-clonic seizures and salivation, but it was intermittently contactable between the seizures, each lasting 10-20 minutes. The dog was restless and seemed confused post-ictally, appeared to be blind, and circled to the left. Further clinical examination revealed generalized lymphadenopathy, decreased proprioception on the right hind limb but no other neurologic abnormalities. However, a complete neurological examination was difficult because the dog was severely stressed and confused. Further diagnostic examinations were planned, but the dog collapsed with pale mucous membranes, cold extremities, not palpable femoral pulse and muffled heart sounds.

Ultrasound showed a tumor in the spleen and hemorrhage to the abdominal cavity. The dog was euthanized.

Gross Pathology:

The carcass was pale. In the abdomen there was 600 mL non-coagulated blood. The source of the blood was identified as a ruptured splenic tumor, 3 cm in diameter. An approximately 8 cm large coagulum was present over the rupture.
The dog had several enlarged lymph nodes, e.g. the right iliofemoral and the hepatic lymph nodes were both 3 cm in diameter, and the right prescapular lymph node was 2 cm in diameter.

A 1.5 cm in diameter tumor was located dorsally in the left hemisphere of the cerebrum. The tumor was well demarcated ventrally, but rostral and caudal transition to normal brain tissue was poorly demarcated. The tumor had a light, red-grey cut surface with multifocal small dark foci (hemorrhage). The tumor compressed surrounding brain tissue.

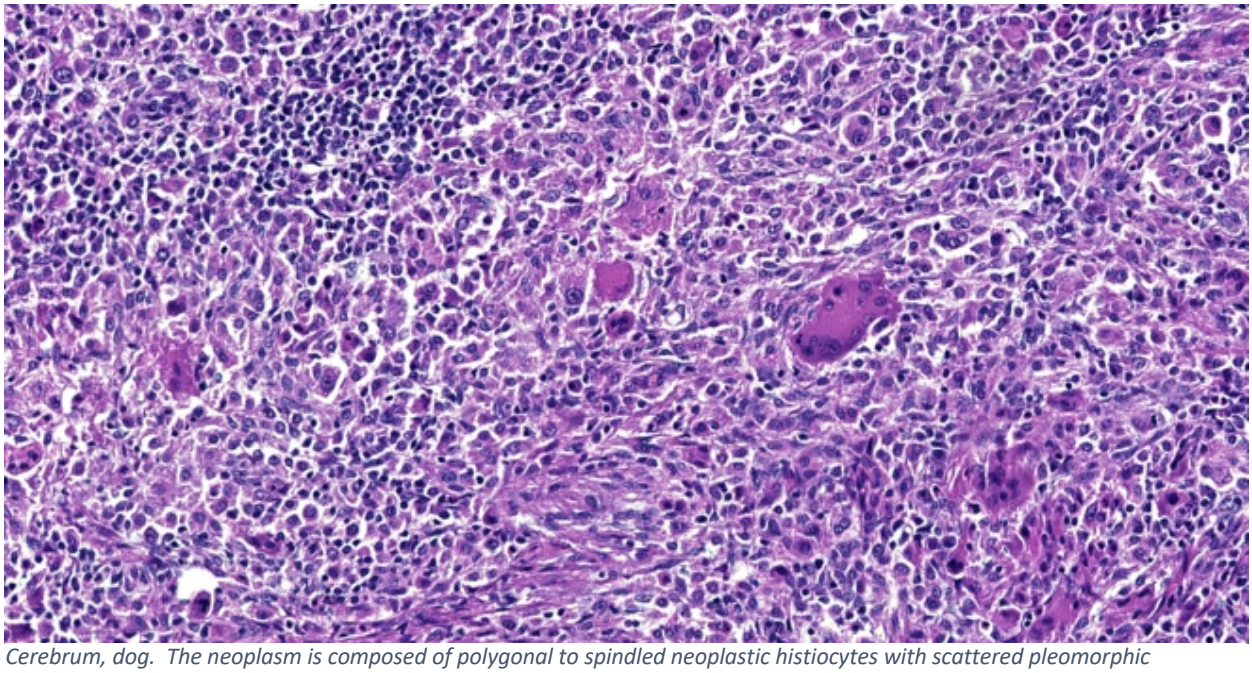

Cerebrum, dog. The neoplasm is composed of polygonal to spindled neoplastic histiocytes with scattered pleomorphic multinucleated cells. Numerous lymphocytes are present within the neoplasm as well. (HE, 310X)

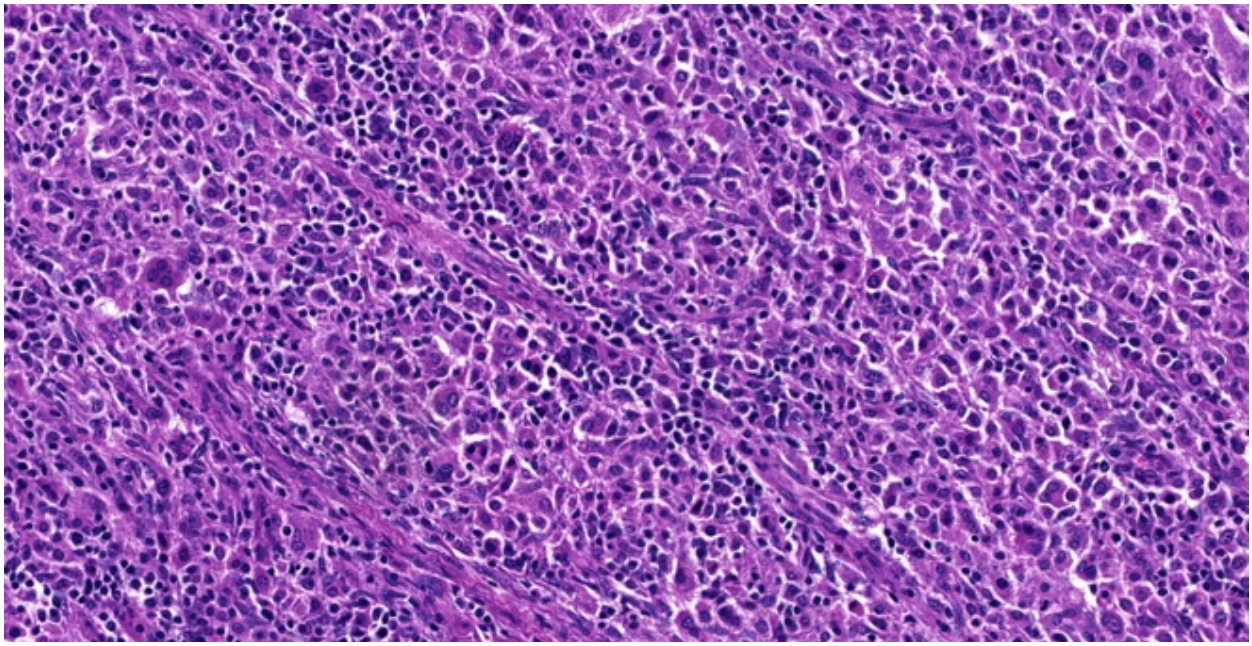

Cerebrum, dog. Some areas of the neoplasm in proximity to the meninges contain trabeculae of fibrovascular tissue. (HE, 310X)

Laboratory results:
None.

Microscopic description:
Dorsally in the left cerebral hemisphere, occupying grey and white matter and involving the overlying leptomeninges, there is a large (2 x 1.5 cm), densely cellular, moderately demarcated, infiltrative, non-encapsulated tumor. The tumor consists of sheets with closely packed round tumor cells, with some areas consisting of spindle cells. The tumor cells are pleomorphic, large with distinct borders, variable amounts of eosinophilic cytoplasm, a round or oval, often eccentric nucleus with coarsely stippled chromatin and 1-3 medium sized to large basophilic nucleoli. There is severe anisocytosis and anisokaryosis and multiple large multinucleated tumor cells and scattered uni- or multinucleated cells with karyomegaly. There are 4 mitotic figures per 10 HPF. In the periphery, there is infiltrative growth, especially along vessels. In the leptomeninges, the tumor cells infiltrate some distance from the main mass. In one of the sections there are multifocal necrotic areas infiltrated by neutrophils. Multifocally in the tumor and associated with vessels, there are infiltration of numerous well-differentiated lymphocytes and some plasma cells. Peri-tumoral brain tissue was compressed with edema, multifocal hemorrhages and prominent vessels.

Immunohistochemical investigation showed that the tumor cells were CD18 positive. The lymphocyte population was composed of both CD3 and CD79 positive cells, thus a mixture of T-lymphocytes and B-lymphocytes.

In enlarged lymph nodes and the ruptured splenic tumor, there was an infiltrative growth of medium sized, relatively homogeneous lymphoid cells that effaced normal tissue architecture, diagnosed as lymphoma.

Contributor's morphologic diagnosis:
Brain: histiocytic sarcoma

Contributor's comment:
The present case is an example of localized, primary central nervous system (CNS) histiocytic sarcoma in a 9 years old female Flat Coated Retriever dog.

Histiocytic sarcoma is a malignant tumor. It is one of several histiocytic diseases that may occur in dogs and cats, a group of proliferative diseases that include lesions thought to be reactive inflammatory lesions, and benign and malignant tumors. The diseases are divided in two groups

based on cell of origin; diseases of Langerhans cell (LC) origin and diseases of interstitial dendritic cell (DC) or macrophage origin. The first group, the diseases of LC origin, include canine cutaneous histiocytoma, canine cutaneous LC histiocytosis and feline pulmonary LC histiocytosis. The second group, of DC or macrophage origin, is again divided in two groups; the histiocytic sarcoma complex which includes several distinctive histiocytic sarcoma syndromes, and the canine reactive histiocytosis which include cutaneous histiocytosis and systemic histiocytosis.[6]

Histiocytic sarcomas are histologically composed of sheets of large, pleomorphic, mononuclear and multinucleated giant cells usually with marked atypia. Some lesions may also consist of spindle shaped cells, either alone or mixed with the other cell type. CNS histiocytic sarcoma also commonly contain large numbers of mixed inflammatory cells (lymphocytes, histiocytes, and plasma cells).[6] All of these morphologic criteria were met in the present case and the tumor cells were confirmed CD18 positive by immunohistochemistry.

The Flat Coated Retriever is one breed predisposed to histiocytic sarcomas, other predisposed breeds are the Bernese Mountain dogs, Rottweilers and Golden Retrievers, however the disease may occur in any breed.[6] Miniature Schnauzers have also been suggested to be predisposed to the disease.[4]

Histiocytic sarcomas may be localized or disseminated. The primary lesion may be solitary or multiple within an organ, and may occur in many different organs, e.g. spleen, lymph node, bone marrow, CNS, skin and subcutis, and periarticular or articular tissues.[6]

CNS involvement in histiocytic sarcoma may arise as a primary location or as a result of metastasis from another location.[6] Although DCs, the cells of origin, may be present in diseased brain tissue, they are not present in normal steady state brain parenchyma, however they do exist in the meninges and choroid plexus.[2] The CNS histiocytic sarcoma usually present as a subdural focal mass, however diffuse meningeal infiltrates

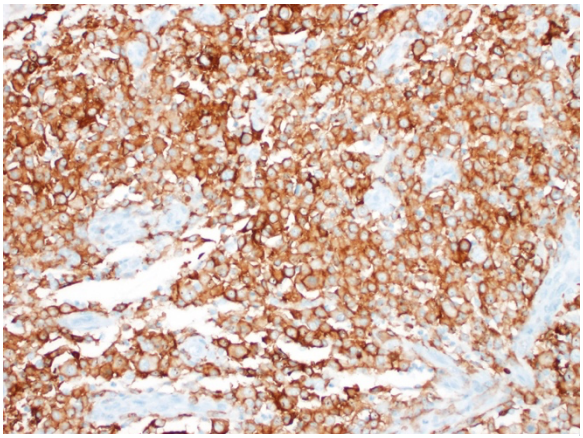

Cerebrum, dog. Neoplastic cells stain strongly immunopositive for IBA-1. (anti-IBA-1, 400X)

may also occur.[6] Although the brain tumor in the present case extended deep into the brain tissue, it infiltrated (and likely originated from) the leptomeninges. In some slides, neoplastic meningeal infiltrates extended deep in sulci next to the tumor.

As reviewed by Moore in 2014, CNS histiocytic sarcomas has not been shown to metastasize extracranially.[6] In a case series describing histiocytic sarcoma with CNS involvement in 19 dogs, 15 of the dogs had histiocytic sarcoma restricted to the CNS and in 4 dogs the CNS involvement was considered as a part of a disseminated multiorgan process.[5] Another study examined the histochemical and immunohistochemical characteristics of primary intracranial canine histiocytic sarcomas of 23 dogs.[10] All cases were considered to be the localized form, although the study was based on only 3 autopsies while the remaining 20 dogs were diagnosed using biopsy material. Tumors located in the brain may be found in different areas of the brain,[5,10] and in the spinal cord, they may be located in any spinal cord segment.[5] There are also case reports describing CNS histiocytic sarcoma together with solitary pulmonary lesions.[1,3]

The dog also had moderate lymphadenomegaly and a ruptured mass in the spleen, the latter being the origin of hemoabdomen. These latter lesions had a morphology consistent with lymphoma, and it was concluded that the dog had two tumor types, both a primary localized CNS histiocytic

sarcoma and a multicentric lymphoma in the spleen and lymph nodes. No metastasis from the brain lesions consistent with malignant histiocytes could be detected in any other tissues examined histologically. The lymphocytic infiltration in the brain tumor was a mixture of B- and T-lymphocytes, interpreted as reactive lymphocytic infiltration, and not metastasis of lymphoma from the lymph nodes or spleen to the CNS.

As a differential diagnosis, another lesion consisting of histiocytic cells together with other inflammatory cells that may present as a single space-occupying lesion is the focal form of granulomatous meningoencephalitis (GME). This form of GME is most commonly located within the white matter of the cerebrum, cerebellum, caudal brainstem or cervical spinal cord, but may also be observed in grey matter. The leptomeninges and choroid plexus may also be involved.[7] It remains controversial whether the focal form of GME represents an immunoproliferative process or a neoplasia.[11] The severe atypia in the present case, however, lead to the diagnosis of a cerebral histiocytic sarcoma rather than the focal form of GME.

Contributing Institution:
Norwegian University of Life Sciences
Faculty of Veterinary Medicine
PO Box 8146 Dep
0033 Oslo
Norway

JPC diagnosis:
Cerebrum: Histiocytic sarcoma, flat coated retriever, canine.

JPC comment:
The contributor summarizes the topic succinctly, and correctly highlights many important points about the disease. In the human literature, there have been very few cases of primary CNS histiocytic sarcoma, with all histiocytic sarcomas comprising less than 1% of all hematolymphoid neoplasms.[12] According to the most recent WHO classification of hematopoietic and lymphoid tissues (2017), a diagnosis of histiocytic sarcoma may be made only when there is expression of one or more histiocytic markers, which include CD163, CD68, or lysozyme, with concurrent lack of expression of CD1a, langerin (Langerhan cells), CD21, CD35 (follicular dendritic cells), CD13, or MPO (myeloid cells).[9] While veterinary diagnoses of histiocytic sarcomas are not in doubt, rarely is immunohistochemical staining performed to rule out other neoplasms of histiocytic origin.

The most recent case report of primary CNS histiocytic sarcoma in humans described a diffuse leptomeningeal neoplasm, filling the subarachnoid space of the brain and spinal cord, with few foci of infiltration into neuroparenchyma. This case had no lymphadenopathy, splenomegaly, hepatomegaly, or cutaneous lesions, increasing the likelihood that this histiocytic sarcoma arose in the leptomeninges as a primary pathology.[12]

The contributor posited one potential differential diagnosis (GME), but others may include Langerhans cell histiocytosis, Rosai-Dorfman disease, and juvenile xanthogranuloma. Histiocytes in Langerhans cell histiocytosis typically exhibit minimal nuclear atypia, are positive for CD1a, and are accompanied by eosinophilic infiltration. Rosai-Dorfman disease is characterized by emperipolesis, infiltration by numerous plasma cells, and histiocytes with abundant amphophilic cytoplasm, round nuclei, and prominent nucleoli. Juvenile xanthogranuloma, there is significant lipidization of histiocytes, also with minimal atypia. Other neoplasms that can be distinguished from histiocytic sarcoma through morphology and immunohistochemistry include glioblastoma, pleomorphic xanthoastrocytoma, and anaplastic large cell lymphoma.[8]

References:

1. Barrot AC, Bédard A, Dunn M. Syndrome of inappropriate antidiuretic hormone secretion in a dog with a histiocytic sarcoma. *Can Vet J.* 2017;58:713-715.
2. D'Agostino PM, Gottfried-Blackmore A, Anandasabapathy N, Bulloch K. Brain dendritic cells: biology and pathology. *Acta Neuropathol.* 2012;124:599-614.
3. Hicks J, Barber R, Childs B, Kirejczyk SGM, Uhl EW. Canine histiocytic sarcoma presenting as a target lesion on brain

magnetic resonance imaging and as a solitary pulmonary mass. *Vet Radiol Ultrasound.* 2017; https://doi.org/10.1111/vru.12502
4. Lenz JA, Furrow E, Craig LE, Cannon CM. Histiocytic sarcoma in 14 miniature schnauzers – a new breed predisposition? *J Small Anim Pract.* 2017;58: 461-467.
5. Mariani CL, Jennings MK, Olby NJ, et al. Histiocytic sarcoma with central nervous system involvement in dogs: 19 cases (2006–2012). *J Vet Intern Med.* 2015;29:607-613.
6. Moore PF. A Review of histiocytic diseases of dogs and cats. *Vet Pathol.* 2014;51:167-184.
7. O'Neill EJ, Merrett D, Jones B. Granulomatous meningoencephalomyelitis in dogs: A review. *Ir Vet J.* 2005;58:86-92.
8. So H, Kim SA, Yoon DH, et al. Primary histiocytic sarcoma of the central nervous system. *Cancer Res Treat*. 2015;47(2):322-328.
9. Swerdlow SH, Campo E, Harris NL, Jaffe ES, Pileri SA, Stein H, Thiele J (Eds): *WHO Classification of Tumours of Haematopoietic and Lymphoid Tissues* (Revised 4th edition). IARC: Lyon 2017.
10. Thongtharb A, Uchida K, Chambers JK, Kagawa Y, Nakayama H. Histological and immunohistochemical studies on primary intracranial canine histiocytic sarcomas. *J Vet Med Sci.* 2016;78:593-599.
11. Vandevelde M, Higgins RJ, Oevermann A. Inflammatory diseases. In: Vandevelde M, Higgins RJ, Oevermann A eds. *Veterinary neuropathology, essentials of theory and practice.* 1st ed. West Sussex, UK: John Wiley & Sons; 2012:48-80.
12. Zanelli M, Ragazzi M, Marchetti G, et al. Primary histiocytic sarcoma presenting as diffuse leptomeningeal disease: Case description and review of the literature. *Neuropathology*. 2017;37(6):517-525.

CASE 4: Case 2 (4101228-00)

Signalment: Bovine, 4-week-old intact male Friesian calf (*Bos taurus*)

History:
The 4-week-old Friesian bull calf was one of a mob of 50 calves bought into a calf-rearing facility, from an unknown dam and sire. The calf presented with a swollen scrotum with palpable masses and marked abdominal distension. The calf was in fair body condition, with a normal demeanor and appetite, and no evidence of weakness. Abdominocentesis revealed a serosanguinous peritoneal effusion. The fluid was not submitted for analysis and euthanasia was elected.

Gross Pathology:
Gross pathological findings included multifocal to coalescing, 2mm-6cm, pink to white nodules scattered over the serosal surface of the abdominal viscera, which extended through the inguinal canal, and were widely dispersed over the tunica vaginalis of the left and right testes. There was gelatinous edema of the scrotal epidermis and tunica dartos, as well as 8-10L of serosanguinous peritoneal effusion, which contained numerous fibrin clots.

Laboratory results:
Immunohistochemistry revealed strong positive cytoplasmic immunoreactivity for pancytokeratin antibody clone AE1/AE3. Low numbers of individual or clustered neoplastic cells reacted with the anti-vimentin antibody (clone V9).

Microscopic description:
Sections of the forestomachs and spleen were examined histologically. Extending from the serosa of the spleen and forestomachs is a poorly

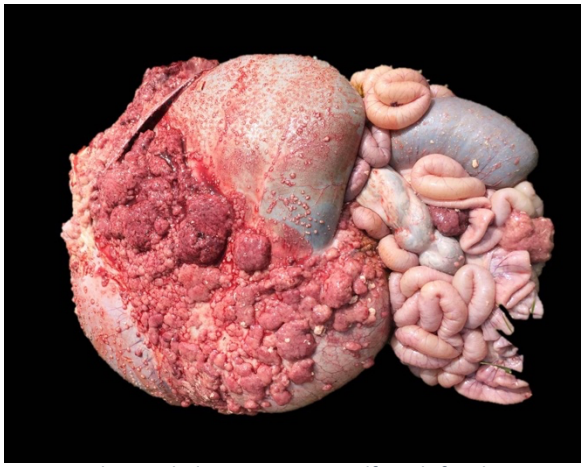

Peritoneal mesothelioma, Friesian calf, multifocal to coalescing, variably-sized nodules scattered over the serosal surface of the abdominal viscera. (Photo courtesy of the Institute of Veterinary Animal and Biomedical Sciences, Massey University, New Zealand)

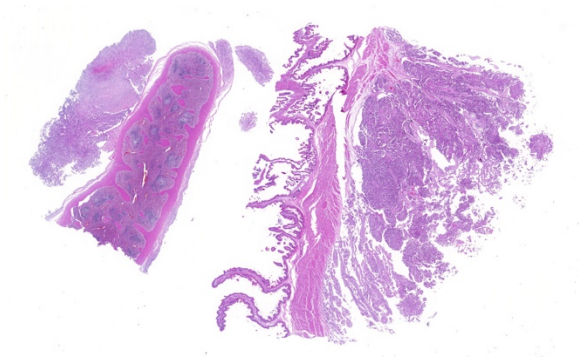

Spleen, reticulum, calf. Subgross magnification of the tissues submitted for examination. At low magnification, a papillary neoplasm extends outward from both tissues. (HE, 5X)

demarcated, unencapsulated, highly cellular population of neoplastic mesothelial cells forming papillary and micropapillary projections, supported by a fine fibrovascular stroma. Neoplastic cells are pleomorphic, polygonal to spindle-shaped, with variably distinct cell borders, a moderate amount of eosinophilic, often vacuolated cytoplasm, round to ovoid central nuclei, vesicular to stippled chromatin and 1-3 nucleoli. There is moderate anisocytosis and anisokaryosis and rare multinucleated cells (up to 4 variable sized nuclei) with evidence of nuclear molding. The mitotic rate is 2 per 40X HPF. Scattered neoplastic cells are hypereosinophilic, shrunken and have pyknotic nuclei (necrosis). There are occasional small aggregates of lymphocytes and rare neutrophils scattered through the neoplastic cells.

Contributor's morphologic diagnosis:
Rumen and spleen: Peritoneal mesothelioma, epithelioid, Friesian, Bovine.

Contributor's comment:
Mesotheliomas are rare in all domestic animals, most commonly reported in cattle and notable as a congenital tumor of calves. They are also described in dogs, cats, horses, rats, and more recently in wildlife species including skunks, Amazon Parrots and jaguars. [8,9,14]

Mesotheliomas may arise on the pleura, pericardium, and peritoneum (including tunica vaginalis of the testes). Most bovine mesotheliomas are peritoneal, with ascites as the primary presenting clinical sign.[12] In fetal cases, this can lead to dystocia.[10] Congenital tumors have been described as those discovered in fetuses or in calves younger than two months of age.[11]

Mesothelial cells secrete serous fluid,[3] as well as performing homeostatic and innate immune functions. Mesotheliomas spread readily by seeding, so are usually considered malignant,[12] although lymphatic metastasis and direct invasion also occur. Scrotal tunica vaginalis involvement is reported in rats, dogs, humans and bulls, including rare historical reports of congenital cases in calves.[1]

Histological classifications include epithelioid (cuboidal cells forming papillary projections over a fibrovascular core), sarcomatous (spindle-shaped cells) and biphasic (mixed) patterns. Epithelioid tumors are further divided in animals into those with non-neoplastic scirrhous proliferation with sparse neoplastic mesothelial cells (sclerosing mesotheliomas), or those predominantly composed of neoplastic cells forming cystic, tubular, solid, deciduoid or papillary structures.[12] Papillary is the most common subtype. The stroma can have chondroid or osseous differentiation, evidence of the multipotency of mesothelial cells.[6]

Differential diagnoses include metastatic carcinoma and hyperplastic (reactive) mesothelium. It is very difficult to distinguish between mesothelioma and hyperplasia cytologically,[12] because reactive mesothelial cells can share the large nucleoli, binucleation and mitotic figures of their neoplastic counterparts. Mesotheliomas may have indistinct vacuoles,

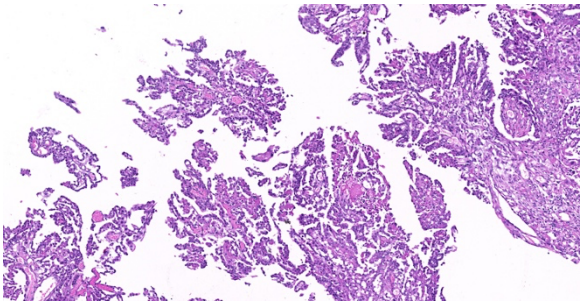

Serosa, reticulum, calf. Higher magnification demonstrating the papillary nature of the neoplasm. (HE, 15X)

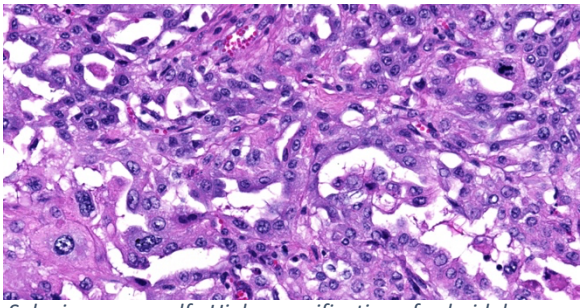

Splenic serosa, calf: High magnification of cuboidal neoplastic cells lining papillary projections, with marked anisokaryosis and anisocytosis. (HE, 400X)

compared to crisper vacuoles suggestive of adenocarcinoma.[4] Similar to adenocarcinomas, histologically epithelioid mesotheliomas form tubules, papillae, trabeculae and can form pseudoacini containing basophilic extracellular material. If these cells have columnar shape and eccentric nuclei, adenocarcinoma should be considered.

Mesotheliomas secrete Alcian-Blue-positive hyaluronic acid in their cytoplasm and stromal matrix. After removal by pre-treatment with hyaluronidase, this delineates mesothelioma from adenocarcinoma (which remains Alcian-blue-positive, due to its neutral mucin).

Immunohistochemical staining of mesotheliomas is positive for cytokeratin 18 and vimentin. Calretin positivity indicates likely mesothelioma (particularly biphasic) over adenocarcinoma, along with carcinoembryonic antigen negativity (CEA- human only).

Ultrastructure is also helpful in distinguishing between carcinoma and many mesotheliomas, because epithelioid mesotheliomas have plentiful, long, sometimes branching microvilli over most of their surface, and circumferential nuclear intermediate microfilaments, whereas adenocarcinomas (while they share desmosomes and tight junctions) have few to absent microvilli and no perinuclear microfilaments.[6]

In humans, mesothelioma is associated with exposure to asbestos, radiation and possibly SV40, and in F344 rats can be induced by vinylidene chloride. Crocodilite, the most oncogenic asbestos fiber, interferes with spindle and chromosome motion in mitosis, which is thought to cause translations, deletions and aneuploidy.[7]

Ferruginous bodies have been identified in the lungs of cattle and dogs with mesothelioma, however in many other domestic animal cases there were no asbestos bodies and no historical exposure. Asbestos bodies can be difficult to identify by light microscopy.[6]

In F344/N rats, gene expression of spontaneous mesotheliomas showed downregulation of tumor suppressors PTEN and TP53 and GADD45, along with overexpression of an anti-apoptotic BCl mediator (Bcl12a1) and downregulation of pro-apoptotics BAX, and Fadd and Fas mediators. These rats also had upregulation of growth factors TGFα and TGF β, IGF, p38MAPK and NFKB. Interestingly, there was also paradoxical downregulation of cell cycle mediators MYC and JUN.[2]

Contributing Institution:
Massey University
Institute of Veterinary, Animal and Biomedical Sciences
Private Bag 11 222
Palmerston North 4442
New Zealand

JPC diagnosis:
Serosa, reticulum and spleen: Mesothelioma, papillary type, Friesian, bovine.

JPC comment:
There may be tissue variation between slides. The images captured at JPC were from the affected

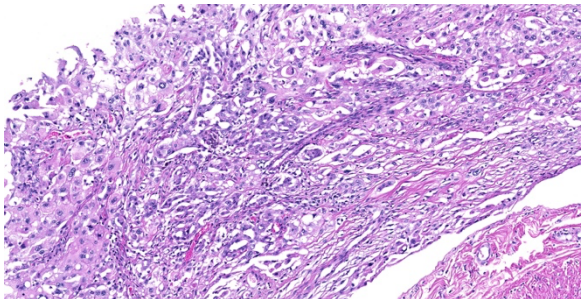

Splenic serosa, calf: In this area, the fibrous stroma is dense, with neoplastic cells forming nests and packets within it. (HE, 125X)

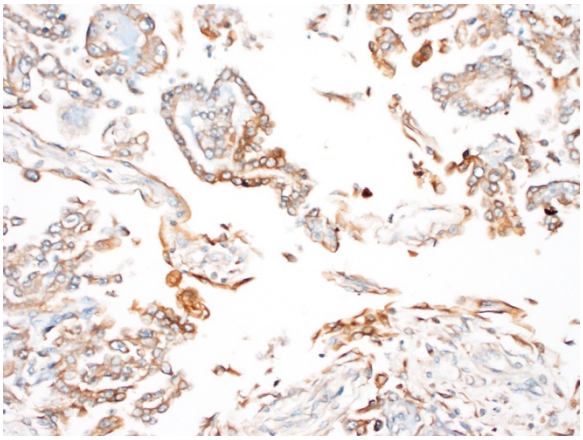

Serosa, reticulum, calf: Neoplastic cells stain strongly positive for cytokeratin. (anti-AE1-AE3, 400X)

reticulum, but there may be slides of rumen as well.

The contributor provides a concise narrative about mesothelioma and touches on some of the molecular pathogenesis of this disease. A Disintegrin And Metalloprotease (ADAM) transmembrane proteases, and specifically ADAM10, are overexpressed in several cancers. A critical aspect of ADAM10 is its sheddase activity, which can cleave growth factors, receptors, and adhesion proteins, which each play important roles in tumor progression. ADAM10 can cleave CD44, E-cadherin, N-cadherin, and L1 adhesion molecules, an ability correlated with neoplastic cell migration and invasion. Using *in vivo* mouse models, using siRNA to deplete ADAM10, migration of malignant mesothelial cells was decreased, presenting a potential treatment strategy.[13]

Ferroptosis is a pathway of cellular death that involves iron-dependent lipid peroxidation, with glutathione peroxidase 4 (GPX4) the central regulator. Dysregulation of ferroptosis has been implicated in ischemic organ damage and cancer. Inhibition of GPX4 can directly facilitate ferroptosis, which contributes to the antitumor function of p53, BAP1, and fumarase. Ferroptosis can be regulated by cadherin-mediated NF2 and Hippo signaling pathways. Interruption of these pathways allows the proto-oncogenic transcriptional co-factor YAP to promote ferroptosis. A recent mouse model of malignant mesothelioma showed that inactivation of NF2 rendered neoplastic cells more sensitive to ferroptosis, revealing the NF2-YAP signaling as a potential area of treatment.[15]

In the field of artificial intelligence, classification is one of the most basic tasks performed regularly. One simple example of classification is the spam filter used to classify emails using natural language processing and other characteristic signatures. A neural network is a series of nodes between an input and output, with weights associated with transitions between nodes. The end result is a model that will classify the input into designated output categories. There is tremendous efficiency and capability variation of neural networks determined by the number of nodes, forward or backward propagation, supervised versus unsupervised learning, and other statistical differences. Often the different nodes, or groups of nodes, can be correlated to specific decision criteria. A French research project, MesoNet, leveraged the data from MESOBANK and created a neural network to classify whole slide images of malignant mesotheliomas in humans. They were able to correlate decision points to histologic features, such as inflammation in the stroma, cellular diversity, and vacuolization. By correlating the classifications with patient mortality data, it was determined that the model was more accurate in predicting patient survival than current pathology practice. While nearly 3000 cases of independent malignant mesotheliomas were required to build

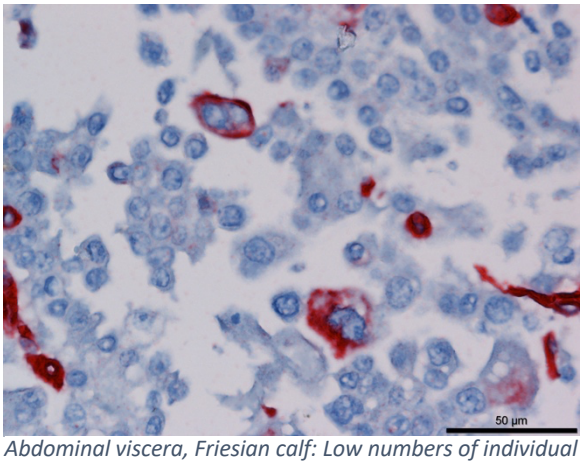

Abdominal viscera, Friesian calf: Low numbers of individual or clustered neoplastic cells reacted with the anti-vimentin antibody (clone V9) (Vim clone V9 40X) (Photo courtesy of the Institute of Veterinary Animal and Biomedical Sciences, Massey University, New Zealand)

this neural network, if overtraining is avoided, models such as this may have sufficient transportability for use in other facilities and other datasets.[5]

References:

1. Baskerville A: Mesothelioma in calf. *Pathologia Veterinaria* 1967:4(2)**:**149-+.
2. Blackshear PE, Pandiri AR, Ton T-VT, Clayton NP, Shockley KR, Peddada SD, et al.: Spontaneous Mesotheliomas in F344/N Rats are Characterized by Dysregulation of Cellular Growth and Immune Function Pathways. *Toxicologic pathology* 2014:42(5)**:**863-876.
3. Brower A, Herold LV, Kirby BM: Canine Cardiac Mesothelioma with Granular Cell Morphology. *Veterinary Pathology* 2006:43(3)**:**384-387.
4. Butnor KJ: My approach to the diagnosis of mesothelial lesions. *Journal of Clinical Pathology* 2006:59(6)**:**564-574.
5. Courtiol P, Maussion C, Moarii M, et al. Deep learning-based classification of mesothelioma improves prediction of patient outcome. *Nature Medicine*. 2019;25:1519-1525.
6. Head KW: *Histological classification of tumors of the alimentary system of domestic animals*: Published by the Armed Forces Institute of Pathology in cooperation with the American Registry of Pathology and the World Health Organization Collaborating Center for Worldwide Reference on Comparative Oncology, 2003.
7. Jeffrey G. Ault RWC, Cynthia G. Jensen, Lawrence C. W. Jensen, Lori A. Bachert, and Cozily L Rieder: Behavior of Crocidolite Asbestos during Mitosis in Living Vertebrate Lung Epithelial Cells. *CancerResearch* 1995:55**:**792-798.
8. Kim S-M, Oh Y, Oh S-H, Han J-H: Primary diffuse malignant peritoneal mesothelioma in a striped skunk (Mephitis mephitis). *Journal of Veterinary Medical Science* 2016:78(3)**:**485-487.
9. McCleery B, Jones MP, Manasse J, Johns S, Gompf RE, Newman S: Pericardial Mesothelioma in a Yellow-naped Amazon Parrot (Amazona auropalliata). *Journal of Avian Medicine and Surgery* 2015:29(1)**:**55-62.
10. Misdorp W: Congenital tumours and tumour-like lesions in domestic animals. 1. Cattle - A review. *Veterinary Quarterly* 2002:24(1)**:**1-11.
11. Misdorp W: Tumours in calves: Comparative aspects. *Journal of Comparative Pathology* 2002:127(2-3)**:**96-105.
12. Munday JS, Löhr CV, Kiupel M: Tumors of the Alimentary Tract *Tumors in Domestic Animals*: John Wiley & Sons, Inc.; 2016: 499-601.
13. Sepult C, Bellefroid M, Rocks N, et al. ADAM10 mediates malignant pleural mesothelioma invasiveness. *Oncogene*. 2019;38:3521-3534.
14. Souza FDL, de Carvalho CJS, de Almeida HM, Pires LV, Silva LD, Costa FAL, et al.: Peritoneal mesothelioma in a jaguar (Panthera onca). *Journal of Zoo and Wildlife Medicine* 2013:44(3)**:**737-739.
15. Wu J, Minikes AM, Gao M, et al. Intercellular interaction dictates cancer cell ferroptosis via NF2-YAP signalling. *Nature*. 2019;572:402-406.